

# Temporal separation of whale vocalizations from background oceanic noise using a power calculation

Jacques van Wyk\*, Johan du Preez† and Jaco Versfeld‡

Department of Electrical and Electronic Engineering, University of Stellenbosch  
Stellenbosch, South Africa

Email: \*jvanwyk40@gmail.com, †jadupreez@gmail.com, ‡jaco.versfeld@gmail.com



**Abstract**—The process of analyzing audio signals in search of cetacean vocalizations is in many cases a very arduous task, requiring many complex computations, a plethora of digital processing techniques and the scrutinization of an audio signal with a fine comb to determine where the vocalizations are located. To ease this process, a computationally efficient and noise-resistant method for determining whether an audio segment contains a potential cetacean call is developed here with the help of a robust power calculation for stationary Gaussian noise signals and a recursive method for determining the mean and variance of a given sample frame. The resulting detector is tested on audio recordings containing Southern Right whale sounds and its performance compared to that of an existing contemporary energy detector. The detector exhibits good performance at moderate-to-high signal-to-noise ratio values. The detector succeeds in being easy to implement, computationally efficient to use and robust enough to accurately detect whale vocalizations in a noisy underwater environment.

**Keywords**— Gaussian noise, detection, whale vocalizations, power, variance

## 1 INTRODUCTION

When processing and analyzing digital audio signals, it is often practical to extract only the most useful contents of the complete signal. In speech processing there exist many applications where the automatic differentiation between speech and silence proves useful, such as detecting the silence before and after breaths [3]. When analyzing underwater recordings for cetacean calls, where there may be only a few minutes of useful audio data embedded in hours of underwater noise, the necessity for such a detection method becomes abundantly clear. Numerous methods have been proposed for speech detection using statistical models and maximum likelihood estimation [13][14], as well as detection methods developed for marine use [15][16]. There are, however, few methods available that are both easy to implement and computationally inexpensive enough to be used in conjunction with more complex detection or classification methods. What is required is a detection method with relatively simple and powerful statistical calculations that provides effective, computationally efficient and robust performance in the presence of background noise. Such a detector is developed here with the help of a novel power calculation for Gaussian noise signals [11],

to determine the power threshold  $P_{\text{thr}}$  and variance threshold  $Q_{\text{thr}}$ , and a recursive method that is used to calculate the mean and variance [12] of the audio samples. The goal of this paper is to demonstrate the aforementioned detection method in the context of detecting baleen whale vocalizations and compare it to a contemporary energy detection method.

## 2 METHOD

The detailed derivations for the power and recursive calculations are shown in appendix A and B respectively.

### 2.1 Average Noise Power Estimation

The average power of a discrete signal can be expressed as

$$P = \frac{1}{N} \sum_{i=1}^N X_i^2, \quad (1)$$

where  $X_i$  is a random variable that represents the instantaneous amplitude of the signal at sample  $i$ . It is assumed that each  $X_i$  is an independent and identically distributed (IID) Gaussian variable. With this a model of the average power of stationary Gaussian noise can be established in the form of a probability density function (pdf) [5]. The average power and variance of the estimated power are described by

$$\bar{P} = \sigma_X^2 \quad (2)$$

and

$$\sigma_P^2 = 2\sigma_X^4/N. \quad (3)$$

The power of the Gaussian noise signal is assumed to be  $\sigma_X^2$  (see Appendix A). This is estimated from the local minima of the signal in Chapter 2.4.

## 2.2 Variance in Noise Power Estimation

The variance of the estimated power can be derived by first stating that the variance of the average power is estimated as

$$Q = \frac{1}{K} \sum_{k=1}^K (P_k - \bar{P})^2 \quad (4)$$

where  $P_k$  is an independent power estimate from Equation 1 and  $\bar{P}$  the mean estimated power from Equation 2. The expected value and variance of the variance estimate  $Q$  is given by (see Appendix A)

$$\bar{Q} = \frac{2\sigma_X^4}{N} \quad (5)$$

and

$$\sigma_Q^2 = \frac{8(N+6)\sigma_X^8}{N^3K}, \quad (6)$$

with  $K$  the number of independent power estimates and  $N$  the number of samples used in each of those power estimates.

## 2.3 Sound detection

The given audio recording can be written as a digital signal consisting of  $M$  frames that each contain  $N$  samples. Each frame corresponds to a power calculation. Adjacent frames can be grouped together into superblocks of  $K$  frames. These superblocks correspond to a collection of  $K$  power calculations.

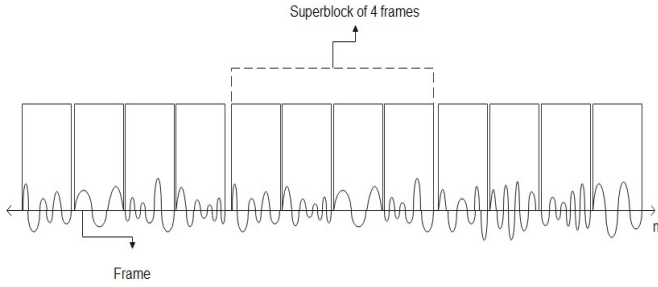


Figure 1: Visual representation of sub-blocks and superblocks

A frame is considered silence if the frame  $x$  consist only of the Gaussian noise signal  $w$ :

$$H_0 : x = w$$

If a segment contains a whale vocalization  $s$  then it is considered a detection:

$$H_1 : x = w + s,$$

where  $x$ ,  $n$  and  $s$  are discrete-time vectors [6]. A suitable threshold model that can discern signals comprised of only noise ( $H_0$ ) from signals that contain possible whale vocalizations ( $H_1$ ) is

$$H = \begin{cases} H_0, & \text{if } P_k < P_{\text{thr}} \text{ and } Q_k < Q_{\text{thr}} \\ H_1, & \text{otherwise} \end{cases} \quad (7)$$

where  $P_k$  is the mean and  $Q_k$  the variance of the power calculations in the superblocks. If a frame or power calculation has a mean or variance below the threshold, then the frame fits within the stationary Gaussian noise model, otherwise it is considered a vocalization. This implies that any signal power or variance above the threshold fits the vocalization model, which is not necessarily true, as the detected signal could be some non-stationary noise signal. To decrease the number of false detections, the value of the thresholds can be increased to allow for more frames to be considered silence. This could in turn cause more of the vocalization frames to be labeled as silence segments. The value of the thresholds are defined as

$$P_{\text{thr}} = \bar{P}_{\text{est}} + n_{\text{std}}\sigma_P, \quad (8)$$

and

$$Q_{\text{thr}} = \bar{Q} + n_{\text{std}}\sigma_Q, \quad (9)$$

where  $\bar{P}_{\text{est}}$  is the mean of the estimated power and  $\sigma_P$  the standard deviation of the estimated power.  $\bar{Q}$  is the mean of the estimated superblock variance and  $\sigma_Q$  the standard deviation of the estimated superblock variance.  $n_{\text{std}}$  is a multiple of the standard deviation. The higher the value of  $n_{\text{std}}$ , the less likely a signal segment will be labeled as a vocalization. To determine the mean  $P_k$  and variance  $Q_k$  of each frame and superblock, recursive calculations are used to determine the mean  $m_n$

$$m_n = m_{n-1} + \frac{x_n - m_{n-1}}{n} \quad (10)$$

and variance  $\sigma_n^2$

$$\sigma_n^2 = \frac{n-2}{n-1}\sigma_{n-1}^2 + \frac{n}{(n-1)^2}(x_n - m_n)^2, \quad (11)$$

with  $n = 2, 3, \dots$  and  $m_1 = x_1$ .

## 2.4 Stationarity

To determine the value of the thresholds, a rough estimate of the average noise power  $\sigma_X^2$  is required. An appropriate estimate could be obtained by taking the minimum amplitude value within a certain timeframe  $T$  and then modulating that value to reflect the average noise level within that timeframe. This will result in threshold values that maintain near-constant values over long durations, due to the fact that the background noise is modelled as a stationary random process. Some signals may have noise levels that remain stationary across the whole signal, whilst other signals may have noise levels that change every few seconds or minutes. To find the local minimum  $P_{\text{min}}$ , an erosion filter [4][7] is applied to the sequence of power calculations  $P_k$ . The equation

$$\bar{P}_{\text{est}} = \alpha_f P_{\text{min}} \quad (12)$$

gives us the estimated mean power, where  $\alpha_f$  is the floor modulation coefficient.  $\alpha_f$  should be just large enough that it approximates the noise floor and small enough that crucial low-amplitude signal information isn't lost. A large  $\alpha_f$  value will cause the threshold values to be large as well, which could cause true positives to be disregarded. A good value for  $\alpha_f$  would be 1–10 dB. A dilation filter

can also be used to find the local maximum, if the local minimum is too small. The local maximum would then be divided by a coefficient to approximate the noise level.

It is recommended that some type of impulse filtering algorithm is implemented to remove any unwanted short bursts of non-stationary noise that could be picked up by the detector. A simple way to do this is to remove any detected segment that is shorter than a certain duration.

Because the detector is based on a stationary Gaussian noise model, it will be referred to as the stationary noise on-line (SNO) detector.

### 3 EXPERIMENTS

To test the performance of the SNO detector, audio files containing Southern Right whale (*Eubalaena australis*) vocalizations were put through the detector to determine the precision and recall (true positive rate) [2] of the detector. To gauge the performance of the SNO-detector, RavenPro’s band-limited energy detector (BLED) [9] was used as a comparison tool. The segmentation performance of the detectors were evaluated using Ziólko’s [17] fuzzy segmentation scheme to determine how closely a detected segment matches an annotated segment. The precision  $P$  and recall  $R$  of the detected segments were calculated with

$$P = \frac{|S \cap_{\mu} C|}{S} \quad (13)$$

and

$$R = \frac{|S \cap_{\mu} C|}{C} \quad (14)$$

where  $S$  is the segmentation obtained by the detectors,  $C$  the correct segmentation (as obtained from an annotation text file or csv file),  $|\cdot|$  the duration of the segment and  $\cap_{\mu}$  the intersection between the two sets.

The audio files (Microsoft wav format) used to test the detectors are from a collection of underwater recordings obtained by a hydrophone in the coastal waters of False Bay, South Africa. The audio files have a signal-to-noise ratio (SNR) of 20 dB.

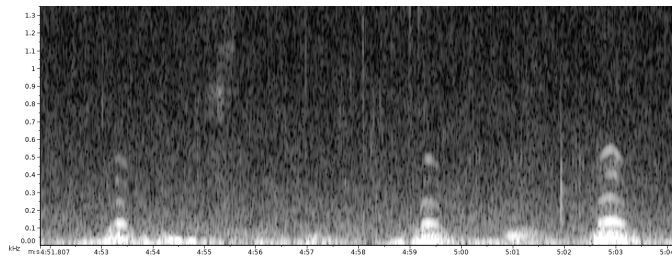


Figure 2: Southern Right Whale sounds

The audio files were downsampled to 8000 Hz and put through an elliptical filter to yield a passband between 100 and 700 Hz. The code was written in C++ with the help of Stellenbosch’s DSP toolkit, which includes the class `onlinesilencedetector.cc` that contains the code to implement the detector as described in Chapter 2.

The parameters of the SNO-detector were determined with training sets that were composed of 10% of the corresponding dataset. After the parameters were tuned, the detector was run on the test set to produce the precision-recall curves.

To gauge how fast both detectors run, a sequence of underwater recordings were put through both detectors and the execution times were measured. The detectors were tested on 11 hours of underwater audio and then on 22 hours of underwater audio. The goal of these experiments were simply to measure execution time, not detection performance.

### 4 RESULTS

The detection performance of the SNO-detector and the BLED are juxtaposed in the precision-recall (P-R) curves below.

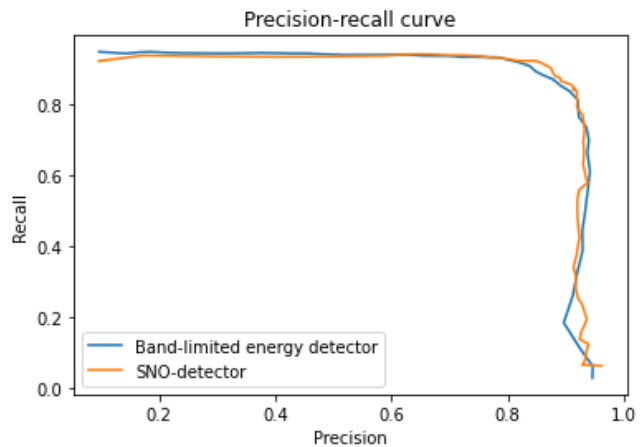


Figure 3: Precision-recall curve of southern right whale calls (SNR: 20 dB)

Both detectors display satisfactory results when applied to the Southern Right Whale (SRW) audio recordings, which has a high signal-to-noise ratio. From Figure 3 it is apparent that both detectors perform similarly at low-to-medium threshold values where the recall is high. As the threshold becomes larger and the recall decreases, the BLED loses some precision until the threshold becomes high enough that most of the false positives are disregarded. The SNO-detector has precision values that increase and decrease at higher threshold values, which would be caused by the detector obtaining shorter vocalization segments as the quieter parts of the segments fall below the power and variance threshold. The precision would then increase as the threshold becomes larger and disregards more false positives.

The results were achieved by configuring the detector parameters, such as the frame sizes and target signal lengths, and then setting the threshold values to have the highest recall (accept the maximum amount of potential detections), after which the threshold is increased until the maximum precision is reached (the maximum false detections are excluded). For the SNO-detector to function properly it’s crucial to select proper values for frame size  $N$ , superblock size  $K$  and stationarity timeframe  $T$ . The effect of different frame values are displayed in Figure 4.

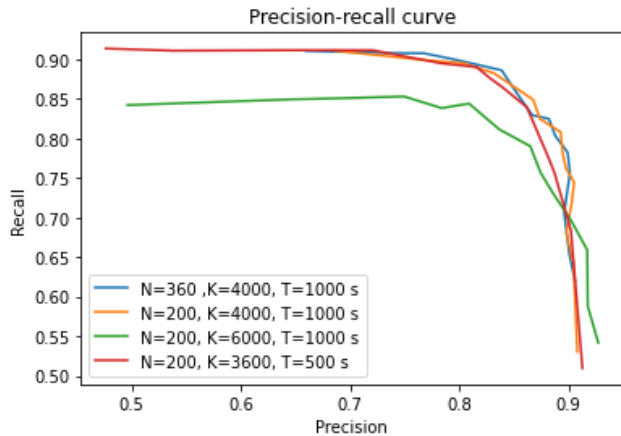


Figure 4: Precision and recall at different values for  $N$ ,  $K$  and  $T$

To gauge the performance of the detectors under low signal-to-noise ratios, the audio files were modified with added Gaussian noise that lowered the SNR of the signals to 10 dB, after which the signals were put through both detectors. The detection results are displayed in Figure 5.

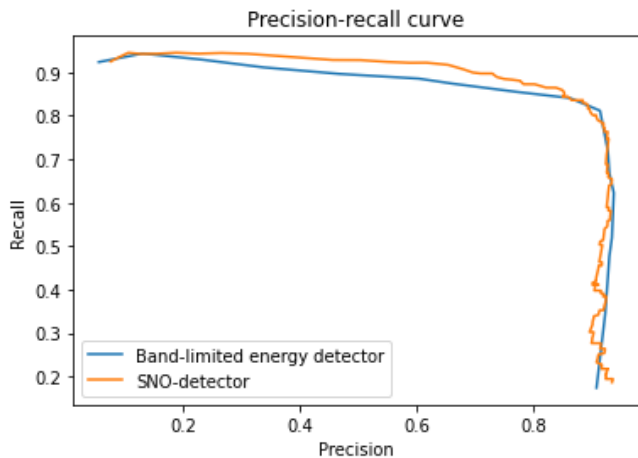


Figure 5: Precision and recall curve of SRW calls (SNR: 10 dB)

Both detectors perform worse in lower signal-to-noise ratios. The curves in Figure 5 display detection behaviours that are similar to those in Figure 3, such as the counter-intuitive decrease in precision at high threshold values. The SNO-detector performs better at lower precision values, but has lower precision as the threshold increases compared to the BLED.

The execution times of both detectors are displayed in Table 1. The execution times do not take into account the reading of audio files, only the detection times.

Table 1: Execution times of SNO-detector and BLED

Audio Duration	Execution time	
	SNO-detector	BLED
11 hours	13 secs	56 secs
22 hours	27 secs	113 secs

From Table 1 it is apparent that the SNO-detector performs 4

times quicker than the BLED. The difference in execution times could be caused by the difference in computational complexity of the detection algorithms. Another factor is the programming language used to code each method. The SNO-detector was written in C++ while Raven Pro was written in Java. It is expected that any application written in Java, a high-level programming language, would run slower compared to an application written in C++. Since the source code for the BLED is not available, it could not be replicated in C++.

## 5 DISCUSSION

As expected, both detectors perform well in high SNR environments. The SNO-detector maintains a good true positive ratio as the threshold and precision increases, as does the BLED. In the recordings a common source of high frequency noise called "shrimp snapping" was observed. Both detectors would filter out the majority of the noise, but there were some loud wideband bursts caused by the shrimp snapping that could be picked up in the whale call bandwidth. These bursts were usually strong enough to be picked up by the detector and not short enough to be disregarded by the impulse filter. This created some false positive results, which is to be expected from an energy detector, as any sound above the power threshold will be regarded as a detection, be it a whale vocalization or noise. The SNO-detector's use of a variance threshold does help to ignore a large portion of background noise and recognize most of the whale calls as true positives, although the stronger bursts of non-stationary noise do cause misdetections.

The length of  $N$  and  $K$  must be carefully selected as they aren't initially self-evident and dictate much of the performance of the SNO-detector. A solution to this could be to optimize the sample sizes with regard to some training data before using it for detection. Another consideration is the proper specification of the calls to be detected, as it is impossible to automatically detect every single call in the audio files [1]. If calls lower than a certain SNR, for example lower than 5 dB, were to be picked up, the precision of the detectors would suffer greatly. It is thus important to consider the type of calls to be detected and the overall background noise of the audio recording to avoid negligible results.

## 6 CONCLUSIONS

When analyzing underwater recordings for cetacean sounds there will almost certainly be noise present, be it from wind, other marine animals, shipping or ice [8]. A capable noise-resistant and effective detection method is required to assist researchers in finding cetacean sounds amidst all this noise, and the stationary noise on-line detector serves this purpose well. The Gaussian power calculations presented here provide a powerful and easily implementable method of modelling the average power and variance of background noise with which an effective and robust detector can be built. In favourable signal-to-noise ratios the SNO-detector can easily differentiate background noise from whale vocalizations, whilst in very noisy environments it occasionally struggles with misdetections and falsely labeling low amplitude signals as silence. The SNO-detector can be used to quickly find cetacean vocalizations before manually refining the results, or as the first step in a speech recognition toolchain.

A potential improvement that can be implemented is in the form of an optimization method to find suitable values for  $N$ ,  $K$  and stationarity duration  $T$  as well as  $\alpha_f$ . If an audio signal has too many bursts of strong noise a correlation-based method could be used in conjunction with the noise detector to filter out these strong noise segments after being picked up.

## APPENDIX A POWER AND POWER VARIANCE IN A STATIONARY GAUSSIAN NOISE SIGNAL

### A density for the estimated average power of Gaussian noise

We model a silence signal (with a certain background noise-level) as a sequence of statistically independent Gaussian random variables  $X_i$  with  $i = 1 \dots N$ , each with mean  $a_X = 0$  and variance  $\sigma_x^2$ .

Firstly we will derive a density function for the estimated average power  $P$  of  $X$ . From this we can determine the mean and variance of  $P$ . Let

$$P = \frac{1}{N} \sum_{i=1}^N X_i^2 \quad (15)$$

be the estimated power. Since the  $X_i$ 's are random variables, so will be  $P$ . We want to find the density  $f_P(p)$ .

First consider the transformation  $Y = X^2$ . Then  $\frac{dy}{dx} = 2x$  and  $x = \pm\sqrt{y}$ .

Using basic theory on the transformation of random variables [10] we find that

$$\begin{aligned} f_Y(y) &= \frac{f_X(x)}{\left|\frac{dy}{dx}\right|} \Big|_{x=-\sqrt{y}} + \frac{f_X(x)}{\left|\frac{dy}{dx}\right|} \Big|_{x=+\sqrt{y}} \\ &= \frac{f_X(x)}{2\sqrt{y}} \Big|_{x=-\sqrt{y}} + \frac{f_X(x)}{2\sqrt{y}} \Big|_{x=+\sqrt{y}} \\ &= \frac{1}{\sqrt{2\pi\sigma_x^2}} y^{\frac{1}{2}-1} e^{-\frac{y}{2\sigma_x^2}} u(y). \end{aligned}$$

Therefore  $Y$  is Gamma distributed with parameters  $b = \frac{1}{2}$  and  $a = \frac{1}{2\sigma_x^2}$ . Its characteristic function is given by:

$$\Phi_Y(\omega) = \left( \frac{\frac{1}{2\sigma_x^2}}{\frac{1}{2\sigma_x^2} - j\omega} \right)^{\frac{1}{2}}.$$

Now consider:

$$Z = \sum_{i=1}^N Y_i \text{ with } Y_i \text{ IID.}$$

The characteristic function of  $Z$  is now given by:

$$\begin{aligned} \Phi_Z(\omega) &= [\Phi_Y(\omega)]^N \\ &= \left( \frac{\frac{1}{2\sigma_x^2}}{\frac{1}{2\sigma_x^2} - j\omega} \right)^{\frac{N}{2}}. \end{aligned}$$

Therefore  $Z$  is also Gamma distributed, but now with parameters  $b = \frac{N}{2}$  and  $a = \frac{1}{2\sigma_x^2}$ .

The corresponding density function of  $Z$  is given by:

$$f_z(z) = \frac{\left(\frac{1}{2\sigma_x^2}\right)^{N/2} z^{N/2-1} e^{-\frac{z}{2\sigma_x^2}} u(z)}{\Gamma(N/2)}.$$

The estimated power is calculated as  $P = Z/N$ . Then  $\frac{dp}{dz} = 1/N$  and  $z = Np$ .

$$\begin{aligned} f_P(p) &= N \frac{\left(\frac{1}{2\sigma_x^2}\right)^{N/2} (Np)^{N/2-1} e^{-\frac{Np}{2\sigma_x^2}} u(p)}{\Gamma(N/2)} \\ &= \frac{\left(\frac{N}{2\sigma_x^2}\right)^{N/2} p^{N/2-1} e^{-\frac{Np}{2\sigma_x^2}} u(p)}{\Gamma(N/2)}. \end{aligned}$$

Therefore, finally, we can conclude that  $P$  is also Gamma distributed, but now with parameters

$$b = \frac{N}{2} \quad (16)$$

and

$$a = \frac{N}{2\sigma_x^2}. \quad (17)$$

From the properties of a Gamma density this also implies that

$$\bar{P} = b/a = \sigma_x^2 \quad (18)$$

and

$$\sigma_P^2 = b/a^2 = 2\sigma_x^4/N. \quad (19)$$

### The mean and variance of an estimate of the variance of the estimated mean power

We now estimate the variance  $Q$  of the above estimate of the average power  $P$ . This is given by

$$Q = \frac{1}{K} \sum_{k=1}^K (P_k - \bar{P})^2 \quad (20)$$

with each  $P_k$  an independent power estimate such as given by Eq 15. From the results of the previous section we know  $P_k$  to be Gamma distributed, and in general we can assume its parameters to be  $a$  and  $b$ . Its mean is given by  $\bar{P} = b/a$  (Eq 18) and its variance by  $\sigma_P^2 = b/a^2$  (Eq 19).

The density of  $Q$  is somewhat involved, therefore we will rather focus on directly finding its mean  $\bar{Q}$  and variance  $\sigma_Q^2$ . First consider:

$$Y = \sum_{k=1}^K (P_k - \bar{P})^2. \quad (21)$$

Since the  $P_k$  terms are statistically independent we can easily find the mean  $\bar{Y}$ :

$$\begin{aligned} E[Y] &= \sum_{k=1}^K E[(P_k - \bar{P})^2] \\ &= K\sigma_P^2 \\ &= Kb/a^2. \end{aligned} \quad (22)$$

The variance of  $Y$  can be determined via its moments around the origin:

$$\begin{aligned} \sigma_Y^2 &= E[Y^2] - \bar{Y}^2 \\ &= E[Y^2] - (Kb/a^2)^2. \end{aligned} \quad (23)$$

An expression for  $E[Y^2]$  is needed:

$$\begin{aligned} E[Y^2] &= E\left[\sum_{i=1}^K (P_i - \bar{P})^2 \sum_{j=1}^K (P_j - \bar{P})^2\right] \\ &= E\left[\sum_{i=1}^K (P_i - \bar{P})^4 + \sum_{i=1}^K (P_i - \bar{P})^2 \sum_{j=1, j \neq i}^K (P_j - \bar{P})^2\right]. \end{aligned}$$

Taking into account that  $P_i$  is independent of  $P_j$  with  $i \neq j$  it now follows that:

$$\begin{aligned} E[Y^2] &= \sum_{i=1}^K E[(P_i - \bar{P})^4] + \sum_{i=1}^K E[(P_i - \bar{P})^2] \sum_{j=1, j \neq i}^K E[(P_j - \bar{P})^2] \\ &= K\mu_4 + \sum_{i=1}^K b/a^2 \sum_{j=1, j \neq i}^K b/a^2 \\ &= K\mu_4 + (K^2 - K)(b/a^2)^2 \end{aligned}$$

with  $\mu_4 = E[(P - \bar{P})^4]$  the 4<sup>th</sup> central moment of  $P$ . Substitute this back into Eq 23 to find

$$\begin{aligned} \sigma_Y^2 &= K\mu_4 + (K^2 - K)(b/a^2)^2 - K^2(b/a^2)^2 \\ &= K[\mu_4 - (b/a^2)^2]. \end{aligned} \quad (24)$$

Using the binomial expression for the power of a sum the required central moment can be determined as:

$$\begin{aligned} \mu_4 &= E[(P - \bar{P})^4] \\ &= E\left[\sum_{n=0}^4 \binom{4}{n} P^n (-\bar{P})^{4-n}\right] \\ &= E[(-\bar{P})^4 + 4P(-\bar{P})^3 + 6P^2(-\bar{P})^2 + 4P^3(-\bar{P}) + P^4] \\ &= m_4 - 4m_3\bar{P} + 6m_2(\bar{P})^2 - 3\bar{P}^4 \end{aligned} \quad (25)$$

with  $m_n$  the  $n$ 'th moment of  $P$  around the origin and  $m_1 = \bar{P}$ . We therefore still need to find expressions for the 2nd up to 4th moments of  $P$  around the origin. This can be done via the characteristic function of  $P$ . In general:

$$m_n = E[P^n] = \frac{d^n \Phi_P(\omega)}{j^n d\omega^n} \Big|_{\omega=0}$$

Therefore:

$$\begin{aligned} \Phi_P(\omega) &= \left(\frac{a}{a - j\omega}\right)^b = (1 - j\omega/a)^{-b} \\ \frac{d\Phi_P(\omega)}{d\omega} &= \frac{jb}{a} (1 - j\omega/a)^{-b-1} \\ \frac{d^2\Phi_P(\omega)}{d\omega^2} &= \frac{j^2 b(b+1)}{a^2} (1 - j\omega/a)^{-b-2} \\ \frac{d^3\Phi_P(\omega)}{d\omega^3} &= \frac{j^3 b(b+1)(b+2)}{a^3} (1 - j\omega/a)^{-b-3} \\ \frac{d^4\Phi_P(\omega)}{d\omega^4} &= \frac{j^4 b(b+1)(b+2)(b+3)}{a^4} (1 - j\omega/a)^{-b-4}. \end{aligned}$$

After simplification we therefore find the required moments around the origin:

$$\begin{aligned} m_2 &= \frac{b(b+1)}{a^2} = \frac{b^2 + b}{a^2} \\ m_3 &= \frac{b(b+1)(b+2)}{a^3} = \frac{b^3 + 3b^2 + 2b}{a^3} \\ m_4 &= \frac{b(b+1)(b+2)(b+3)}{a^4} = \frac{b^4 + 6b^3 + 11b^2 + 6b}{a^4}. \end{aligned}$$

Substitute this into Eq 25 and simplify to find that

$$\mu_4 = \frac{3b^2 + 6b}{a^4}.$$

Substitute this into Eq 24 and simplify:

$$\sigma_Y^2 = K \frac{2b^2 + 6b}{a^4}. \quad (26)$$

We now know  $\bar{Y}$  and  $\sigma_Y^2$  via Eqs 22 and 26, and from Eqs 16 and 17 we know the appropriate values of  $b$  and  $a$ . From Eqs 20 and 21 it follows that  $Q = Y/K$ . After further simplification (standard expectation manipulations) we finally get that:

$$\bar{Q} = \frac{\bar{Y}}{K} = b/a^2 = \frac{2\sigma_X^4}{N} \quad (27)$$

and

$$\sigma_Q^2 = \frac{\sigma_Y^2}{K^2} = \frac{2b^2 + 6b}{a^4 K} = \frac{8(N+6)\sigma_X^8}{N^3 K}, \quad (28)$$

with  $K$  the number of independent power estimates and  $N$  the number of samples used in each of those power estimates.

## APPENDIX B RECURSIVE ESTIMATION OF SAMPLE MEAN AND VARIANCE

### Standard ML Estimates

Consider a sequence of samples, namely  $x_1, x_2, \dots, x_n, \dots$ . Note that for the convenience of having the subscript of a sample also coinciding with the number of samples up to that one, we chose to start at index  $n = 1$ . The standard unbiased ML estimates for the mean and variance based on the first  $n$  samples are given by:

$$m_n = \frac{\sum_{i=1}^n x_i}{n} \quad (29)$$

and

$$\begin{aligned} \sigma_n^2 &= \frac{\sum_{i=1}^n (x_i - m_n)^2}{n-1} \\ &= \frac{\sum_{i=1}^n x_i^2 - \frac{(\sum_{i=1}^n x_i)^2}{n}}{n-1}. \end{aligned} \quad (30)$$

## Recursive Version of Standard ML Estimates

We now want to derive expressions to instead do these estimates recursively. We start by rewriting Eq 29 as

$$\begin{aligned}
 m_n &= \frac{\sum_{i=1}^{n-1} x_i}{n} + \frac{x_n}{n} \\
 &= \frac{n-1}{n} \frac{\sum_{i=1}^{n-1} x_i}{n-1} + \frac{x_n}{n} \\
 &= \frac{n-1}{n} m_{n-1} + \frac{x_n}{n} \\
 &= m_{n-1} + \frac{x_n - m_{n-1}}{n},
 \end{aligned} \tag{31}$$

with  $n = 2, 3, \dots$  and  $m_1 = x_1$ .

We can rewrite Eq 30 as follows:

$$\begin{aligned}
 \sigma_n^2 &= \frac{\sum_{i=1}^{n-1} (x_i - m_n)^2}{n-1} + \frac{(x_n - m_n)^2}{n-1} \\
 &= \frac{n-2}{n-1} \frac{\sum_{i=1}^{n-1} [(x_i - m_{n-1}) - (m_n - m_{n-1})]^2}{n-2} + \frac{(x_n - m_n)^2}{n-1} \\
 &= \frac{n-2}{n-1} \sigma_{n-1}^2 + \frac{(x_n - m_n)^2}{n-1} + (m_n - m_{n-1})^2.
 \end{aligned}$$

For stationary sequences with large  $n$  the last term will approach zero and may (approximately) be omitted. However, this is unnecessary. We can combine the last two terms by substituting  $m_{n-1}$  from Eq 31 and after some simplification get:

$$\sigma_n^2 = \frac{n-2}{n-1} \sigma_{n-1}^2 + \frac{n}{(n-1)^2} (x_n - m_n)^2. \tag{32}$$

Eqs 31 and 32 have an interesting form. Both express varying coefficient single pole IIR filters. The recursion may be initialized by setting  $m_1 = x_1$  and  $\sigma_1^2 = 0$  and starting computation from  $n = 2$ .

## Recursive MAP Estimates

MAP estimation of Gaussian parameters ultimately reduces to an ML estimate extended to also include a number  $N$  of “phantom” samples that on their own precisely corresponds to the prior mean and variance values. The above recursive formulations are very easily extended to include this notion. Instead of initially starting with no prior knowledge, one now simply starts the recursion at  $n = N + 1$  with  $m_N$  and  $\sigma_N^2$  set to the desired prior values.

To understand the role of  $N$  it is instructive to remember that it literally represents a number of imaginary prior observations sampled from the prior distribution. The higher we select  $N$ , the more conservatively our estimate will lean towards the prior distribution. Or said differently, we need more than  $N$  new observations before their effect in the estimate will start to override that of the prior model.  $N$  is our conservatism parameter and therefore inversely related to our learning rate.

Also note that nothing prevents us from specifying different values for  $N^{(m)}$  and  $N^{(\sigma)}$  for the mean and variance estimates, thereby effectively giving them different learning rates.

## ACKNOWLEDGMENT

We would like to thank the National Research Foundation for funding the recording equipment used to capture the audio signals used in our research.

## REFERENCES

- [1] Whitlow Au and Marc Lammers. *Listening in the Ocean*. 01 2016.
- [2] Jesse Davis and Mark Goadrich. The relationship between precision-recall and roc curves. In *Proceedings of the 23rd International Conference on Machine Learning, ICML '06*, page 233–240, New York, NY, USA, 2006. Association for Computing Machinery.
- [3] Takashi Fukuda, Osamu Ichikawa, and Masafumi Nishimura. Detecting breathing sounds in realistic japanese telephone conversations and its application to automatic speech recognition. *Speech Communication*, 98:95–103, 2018.
- [4] J.Y. Gil and R. Kimmel. Efficient dilation, erosion, opening, and closing algorithms. *IEEE Transactions on Pattern Analysis and Machine Intelligence*, 24(12):1606–1617, 2002.
- [5] L. Joseph and Peter M. Lee. Bayesian statistics: An introduction. *The American Statistician*, 47:307, 1989.
- [6] Jonas Philipp Luke, José G. Marichal-Hernández, Fernando Rosa, and Javier Almunia. Real time automatic detection of orcinus orca vocalizations in a controlled environment. *Applied Acoustics*, 71(8):771–776, 2010.
- [7] Petros Maragos. Chapter 13 - morphological filtering. In Al Bovik, editor, *The Essential Guide to Image Processing*, pages 293–321. Academic Press, Boston, 2009.
- [8] Brian Miller, Naysa Balcazar, Sharon Nieuwkirk, Emmanuelle Leroy, Meghan Aulich, Fannie Shabangu, Bob Dziak, Won Sang Lee, and Jong Kuk. An open access dataset for developing automated detectors of antarctic baleen whale sounds and performance evaluation of two commonly used detectors. *Scientific Reports*, 11:806, 01 2021.
- [9] Harold Mills. Geographically distributed acoustical monitoring of migrating birds. *Acoustical Society of America Journal*, 108(5):2582, November 2000.
- [10] Peyton Z. Peebles. Chapter 3 - operations on one random variable - expectation. In Al Bovik, editor, *Probability, random variables and random signal principles*, pages 74–80. McGraw-Hill, Inc, 1980.
- [11] Johan Du Preez. Power and power variance in a stationary gaussian noise signal. personal communication.
- [12] Johan Du Preez. Recursive estimation of sample mean and variance. personal communication, May 2008.
- [13] J. Ramirez, J.C. Segura, C. Benitez, L. Garcia, and A. Rubio. Statistical voice activity detection using a multiple observation likelihood ratio test. *IEEE Signal Processing Letters*, 12(10):689–692, 2005.
- [14] Jong Won Shin, Joon-Hyuk Chang, Hwan Sik Yun, and Nam Soo Kim. Voice activity detection based on generalized gamma distribution. In *Proceedings. (ICASSP '05). IEEE International Conference on Acoustics, Speech, and Signal Processing, 2005.*, volume 1, pages I/781–I/784 Vol. 1, 2005.
- [15] Rustam Stolkin, Sreeram Radhakrishnan, Alexander Sutin, and Rodney Rountree. Passive acoustic detection of modulated underwater sounds from biological and anthropogenic sources. In *OCEANS 2007*, pages 1–8, 2007.
- [16] Ildar R. Urazghildiiev, Christopher W. Clark, Timothy P. Krein, and Susan E. Parks. Detection and recognition of north atlantic right whale contact calls in the presence of ambient noise. *IEEE Journal of Oceanic Engineering*, 34(3):358–368, 2009.
- [17] Bartosz Ziółko. Fuzzy precision and recall measures for audio signals segmentation. *Fuzzy Sets and Systems*, 279:101–111, 2015. Theme: Data, Audio and Image Analysis.